

**Effective quantum dynamics in curved thin-layer systems with inhomogeneous confinement**Guo-Hua Liang <sup>1,\*</sup> and Meng-Yun Lai <sup>2</sup><sup>1</sup>*School of Science, Nanjing University of Posts and Telecommunications, Nanjing 210023, China*<sup>2</sup>*College of Physics and Communication Electronics, Jiangxi Normal University, Nanchang 330022, China*

(Received 15 August 2022; accepted 7 February 2023; published 14 February 2023)

The motion of quantum particles homogeneously constrained to a curved surface is affected by a curvature-induced geometric potential. Here, by extending the thin-layer procedure, we consider the case of inhomogeneous confinement and derive the effective Hamiltonian where an extra effective potential appears. This effective potential is relevant to the ground-state energy perpendicular to the surface and the morphology of the confining potential. Tiny fluctuations in the thickness are envisioned to induce considerable magnitude of the effective potential. To demonstrate the impact of the inhomogeneity, we apply our method to investigate the coherent transport on a cylindrical surface where two helical ditches is imposed on the thickness. Numerical analysis reveals that the inhomogeneity of the confinement significantly affects the transport properties through changing the geometric symmetry of the system. This study develops the method for low-dimensional constrained systems and exhibits the possibility of a new degree of control for waveguiding in nanostructures.

DOI: [10.1103/PhysRevA.107.022213](https://doi.org/10.1103/PhysRevA.107.022213)**I. INTRODUCTION**

With the constant progress of techniques for the synthesis of nanostructures [1–4], much attention is paid to the corresponding descriptions of various dynamics in low-dimensional systems in which different kinds of geometric quantities play important roles. Among these quantities, curvature appeals to many interests since it significantly breaks symmetries associated with space coordinates and often relates the system with general relativity, offering a glimpse into the effect of the strong gravitational field. For example, two-beam interference [5], the evolution of speckle patterns [6], and the phase and group velocities of wave packets [7] and elastic waves [8] on curved surfaces have been investigated experimentally, providing analog models for wave optics in the gravitational fields of black holes, wormholes, and the universe with nonvanishing cosmological constant. Besides, the study of curvature effects covers more and more areas nowadays, such as biological systems [9,10] and pattern dynamics [11–14], semiconductors [15–17], magnetism [18,19], superconductivity [20,21], and phase transition [22], manifesting novel and unfamiliar phenomena compared with planar cases.

For the theoretical description of motions bounded to an arbitrary curved surface, there is a generic procedure to obtain the two-dimensional (2D) effective Hamiltonian or equation called the thin-layer procedure (TLP) or the confining potential approach. This approach is originally introduced for tackling the limiting situation where a quantum particle in three-dimensional (3D) Euclidean space is constrained to a curved surface by a strong confining force [23,24]. It was found that a geometric potential depending on the intrinsic and extrinsic curvature of the surface appears in the effective

equation, which was demonstrated in photonic crystals later [25]. The geometric potential reveals that even the dynamics in the normal direction is “frozen” by the confining potential; it indeed contributes to the tangential dynamics because of the curvature. In light of this, the TLP has been developed and applied to many situations, such as a charged particle in an electric and magnetic field [26–28], Dirac particles [29–31], spin-orbital coupling [32–37] and an electromagnetic field [38–40]. In these studies, in addition to the scalar geometric potential, the curved features lead to more geometric effects associated with the internal degrees of freedom and properties of the confined particles. The TLP was also extended to the case of an arbitrary manifold embedded in a higher-dimensional Euclidean space; it was found that a gauge potential appears in the effective Hamiltonian when the space of states for the direction normal to the surface is degenerate [41–45].

It is noteworthy that most studies on the thin-layer system have considered the case where the confining potential is homogeneous everywhere around the surface. In this work, by generalizing the TLP, we discuss the dynamics of a quantum particle constrained to an arbitrarily curved surface by an inhomogeneous confining potential. This problem is important for two reasons: One is to estimate the influence from the imperfection of the confinement, since it is difficult to ensure that the thickness of the layer is the same everywhere in reality; the other is to offer a new toolbox to manipulate and guide quantum states by designing the feature of the confining potential. In addition to the curvature, the confinement inhomogeneity could bring more possibilities to tune the properties of nanostructures. In optics, the variable thickness of a microstructured waveguide can induce an effective refractive index, which is extracted from the fitting of experimental data [46]. In this work, we analytically show that in quantum mechanics the inhomogeneous confining potential can induce an

\*lianggh@njupt.edu.cn

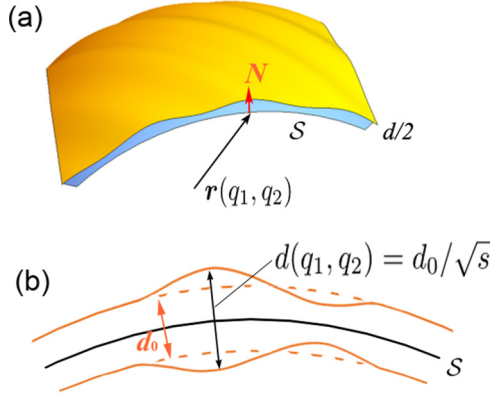


FIG. 1. (a) Schematic picture of a curved layer with inhomogeneous thickness. For clarity, here we show half of the thickness. (b) Schematic diagram of the cross section of the layer in panel (a). The dashed lines give the profile of the layer with homogeneous thickness  $d_0$ .

effective potential totally different from the curvature-induced geometric potential.

The structure of this paper is as follows. In Sec. II, we derive the effective Hamiltonian for particles constrained to an arbitrary curved surface by an inhomogeneous confinement. In Sec. III, we apply this formalism in the case of a cylinder with extra helical confinement force acting on the surface and numerically investigate the transport properties. In Sec. IV, we summarize the conclusions.

## II. EFFECTIVE DYNAMICS

In 3D Euclidean space, the geometry of a curved surface  $\mathcal{S}$  can be described by a position vector  $\mathbf{r}(q_1, q_2)$ , where  $(q_1, q_2)$  are the curvilinear coordinates, as illustrated in Fig. 1(a). To study the quantum mechanics of a spinless particle confined to  $\mathcal{S}$ , we need to describe the portion of space in an immediate neighborhood of  $\mathcal{S}$ . Conventionally in the TLP, the adapted coordinates  $(q_1, q_2, q_3)$  are always chosen to parametrize the space as

$$\mathbf{R}(q_1, q_2, q_3) = \mathbf{r}(q_1, q_2) + q_3 \mathbf{N}(q_1, q_2), \quad (1)$$

where  $\mathbf{N}(q_1, q_2)$  is the unit vector normal to the surface, and  $|q_3|$  gives the distance from the surface. The particle is usually constrained to the surface by a confining potential  $V_c(q_3)$ , which has a deep minimum at  $q_3 = 0$  and is symmetric in the normal direction about its minimum. Such a potential can be expanded as a power series in  $q_3$ ,

$$V_c(q_3) = \frac{m}{2} \omega^2 q_3^2 + O[(q_3)^3], \quad (2)$$

where  $m$  is the particle mass, and the frequency  $\omega$  is an intensity parameter. The leading term of  $V_c$  is a harmonic oscillator potential, which can limit a particle in the range of  $d_c = 2\sqrt{2E_k/m}/\omega$  ( $E_k$  is the kinetic energy) classically. In quantum mechanics, the particle is also found with high probability within the corresponding range, such as  $d_g = 2\sqrt{\hbar/(m\omega)}$  for the ground state. Therefore, we define  $d_0 \propto \sqrt{\hbar/(m\omega)}$  as the thickness of a layer around  $\mathcal{S}$ , such that the thickness is totally

determined by the confining potential  $V_c$ . As  $V_c$  is a function of  $q_3$  only, the thickness is constant along the surface.

With the relation between thickness and the confining potential, it is time to consider the situation of inhomogeneous thickness. Here, we assume that the confining potential can be written as  $U_c(q_1, q_2, q_3) = s^2(q_1, q_2)V_c(q_3)$ , where  $s(q_1, q_2)$  is a dimensionless and continuous function close to unity, which determines the morphology of the potential on  $\mathcal{S}$ . This potential is equivalent to a harmonic oscillator potential with a space-varying intensity  $s\omega$ , accordingly corresponding to a varying thickness  $d(q_1, q_2) = d_0/\sqrt{s}$  [see Fig. 1(b)]. Note that  $U_c$  is still symmetric about the minimum  $q_3 = 0$ .

Taking into account the inhomogeneity of the confining potential, we parametrize the neighborhood space of the surface in the new coordinates  $(q_1, q_2, Q_3)$ , where  $Q_3 = \bar{s}(q_1, q_2)q_3$ , with  $\bar{s}(q_1, q_2)$  being an undetermined function. The new parametrization is then

$$\mathbf{R}(q_1, q_2, Q_3) = \mathbf{r}(q_1, q_2) + \frac{Q_3}{\bar{s}(q_1, q_2)} \mathbf{N}(q_1, q_2). \quad (3)$$

In these coordinates, the irregularities of the confining potential are expected to be absorbed in the normal coordinate  $Q_3$ . Applying this parametrization, we can calculate the covariant components of the three-dimensional metric tensor via  $G_{ij} = \partial_i \mathbf{R} \cdot \partial_j \mathbf{R}$ , with  $i, j = 1, 2, 3$ . From Eq. (3) we obtain

$$\begin{aligned} \partial_a \mathbf{R} &= \partial_a \mathbf{r} + \frac{Q_3}{\bar{s}} [\partial_a \mathbf{N}(q_1, q_2)] + \left[ \partial_a \left( \frac{1}{\bar{s}} \right) \right] Q_3 \mathbf{N}(q_1, q_2), \\ \partial_3 \mathbf{R} &= \frac{1}{\bar{s}} \mathbf{N}(q_1, q_2), \end{aligned} \quad (4)$$

where the index  $a = 1$  and 2 (so does  $b, c$ , and  $d$  in the text below). Since the derivatives of the normal vector  $\mathbf{N}(q_1, q_2)$  lie in the tangent plane of the surface, we have

$$\partial_a \mathbf{N} = \alpha_{ab} \partial_b \mathbf{r}, \quad (5)$$

where  $\alpha_{ab}$  is called the Weingarten curvature matrix. Thus, we obtain all components of the metric tensor  $G_{ij}$ ,

$$G_{ab} = \gamma_{ab} + Q_3^2 \left[ \partial_a \left( \frac{1}{\bar{s}} \right) \right] \left[ \partial_b \left( \frac{1}{\bar{s}} \right) \right] \quad (6)$$

and

$$G_{a3} = G_{3a} = \frac{1}{\bar{s}} \left[ \partial_a \left( \frac{1}{\bar{s}} \right) \right] Q_3, \quad G_{33} = \frac{1}{\bar{s}^2}, \quad (7)$$

where

$$\gamma_{ab} = g_{ab} + \frac{Q_3}{\bar{s}} [\alpha g + (\alpha g)^T]_{ab} + \frac{Q_3^2}{\bar{s}^2} (\alpha g \alpha)_{ab} \quad (8)$$

and  $g_{ab} = \partial_a \mathbf{r} \cdot \partial_b \mathbf{r}$  is the 2D metric tensor for the surface  $\mathcal{S}$ . The determinant of  $G_{ij}$  can also be worked out and the result is  $G = |\gamma|/\bar{s}^2$ .

Further calculation gives the exact form of the inverse of the metric tensor, which turns out to be

$$G^{ij} = \begin{pmatrix} \lambda^{ab} & \lambda^{ac} Q_3 (\partial_c \bar{s}) / \bar{s} \\ \lambda^{bc} Q_3 (\partial_c \bar{s}) / \bar{s} & \bar{s}^2 + Q_3^2 (\partial_c \bar{s}) \lambda^{cd} (\partial_d \bar{s}) / \bar{s}^2 \end{pmatrix}, \quad (9)$$

where  $\lambda^{ab} = (\gamma_{ab})^{-1}$  is the inverse of  $\gamma_{ab}$ .

We can now turn our attention to the derivation of the effective Hamiltonian. The 3D Hamiltonian containing the

confining potential  $U_c$  can be written in the curvilinear coordinates  $(q_1, q_2, Q_3)$  as

$$H_{3D} = -\frac{\hbar^2}{2m}\nabla^2 + s^2 V_c(Q_3/\bar{s}). \quad (10)$$

From Eq. (9), the explicit form of the Laplacian is

$$\begin{aligned} \nabla^2 &= \frac{1}{\sqrt{G}}\partial_i\sqrt{G}G^{ij}\partial_j \\ &= \frac{1}{\sqrt{G}}\partial_3\sqrt{G}[\bar{s}^2 + Q_3^2(\partial_c\bar{s})\lambda^{cd}(\partial_d\bar{s})]\partial_3 \\ &\quad + \frac{1}{\sqrt{G}}\partial_a\sqrt{G}\lambda^{ab}\partial_b + \frac{1}{\sqrt{G}}\partial_a\sqrt{G}\lambda^{ac}Q_3\frac{\partial_c\bar{s}}{\bar{s}}\partial_b \\ &\quad + \frac{1}{\sqrt{G}}\partial_3\sqrt{G}\lambda^{bc}Q_3\frac{\partial_c\bar{s}}{\bar{s}}\partial_b. \end{aligned} \quad (11)$$

The corresponding wave function  $\Phi$  satisfies the normalization condition

$$\int |\Phi|^2\sqrt{G}dq_1dq_2dQ_3 = 1. \quad (12)$$

Our purpose is to get an effective 2D Hamiltonian whose wave function describes the quantum probability density on the surface  $\mathcal{S}$ . Therefore, we need to rescale the 3D wave function  $\Phi$  by  $(|G|/|g|)^{1/4}$ , namely,  $\Psi = (|G|/|g|)^{1/4}\Phi$ , where  $g$  is the determinant of  $g_{ab}$ . The normalization of the new wave function  $\Psi$  is then

$$\int |\Psi|^2dQ_3\sqrt{g}dq_1dq_2 = 1. \quad (13)$$

According to this condition, one can regard  $\int |\Psi|^2dQ_3$  as a probability density for a particle moving on  $\mathcal{S}$  with the curvilinear measure  $\sqrt{g}dq_1dq_2$ . Consequently, the Hamiltonian should also be rescaled as  $H = (|G|/|g|)^{1/4}H_{3D}(|G|/|g|)^{-1/4}$ . By introducing the operators  $\hat{\partial}_a = \partial_a + A_aQ_3\partial_3$ , where  $A_a = \frac{\partial_a\bar{s}}{\bar{s}}$ , the rescaled Hamiltonian can be written in a compact form,

$$\begin{aligned} H &= -\frac{\hbar^2}{2m}[\bar{s}^2G^{-\frac{1}{4}}\partial_3\sqrt{G}\partial_3G^{-\frac{1}{4}} \\ &\quad + (gG)^{-\frac{1}{4}}\hat{\partial}_a\sqrt{G}\lambda^{ab}\hat{\partial}_b(g/G)^{\frac{1}{4}}] + s^2V_c(Q_3/\bar{s}). \end{aligned} \quad (14)$$

Up to now, no approximation has been made. To obtain the effective Hamiltonian, we need to separate the dynamics perpendicular and tangent to the surface, which is associated with the explicit form of the confining potential. Here, we return to Eq. (2) and neglect the terms of order  $(q_3)^3$  and higher, which leads to a harmonic binding form. As a confining potential,  $U_c = \frac{s^2}{2}m\omega^2(Q_3)^2$  must have a large  $\omega$  to ensure the quantum well is deep enough. To evaluate the magnitude of  $\omega$ , following the approach of the TLP, we introduce a small dimensionless parameter  $\epsilon$  and rescale the harmonic frequency as  $\omega \rightarrow \omega/\epsilon$ . Because of the binding, the wave function will be squeezed in a very small range around  $Q_3 = 0$  in the transverse direction. Adopting  $\epsilon$  as a perturbative parameter, we also rescale the normal coordinate as  $Q_3 \rightarrow \sqrt{\epsilon}Q_3$ . In this way,  $U_c$  is of the order  $\epsilon^{-1}$ . The Hamiltonian can be written in powers of  $\epsilon$  as

$$H = H_0 + H_1 + O(\epsilon^{1/2}), \quad (15)$$

where

$$H_0 = \frac{1}{\epsilon}\left[-\frac{\hbar^2}{2m}\bar{s}^2\partial_3^2 + \frac{s^2}{\bar{s}^2}\frac{m}{2}\omega^2(Q_3)^2\right] \quad (16)$$

and

$$H_1 = -\frac{\hbar^2}{2m}\frac{1}{\sqrt{\bar{s}}}\left[\frac{1}{\sqrt{g}}\hat{\partial}_a\sqrt{gg^{ab}}\hat{\partial}_b\right]\sqrt{\bar{s}} + V_g. \quad (17)$$

Here,  $V_g = -\frac{\hbar^2}{2m}(M^2 - K)$  is the well-known geometric potential, with the mean curvature  $M = \text{Tr}(\alpha_{ab})/2$  and the Gaussian curvature  $K = \det(\alpha_{ab})$ . During performing the limit, we have used the fact that  $\sqrt{|\gamma|} = [1 + \text{Tr}(\alpha_{ab})Q_3/\bar{s} + \det(\alpha_{ab})(Q_3)^2/\bar{s}^2]\sqrt{|g|}$ . One may worry about the hermiticity of  $H_1$ , because the expectation of the term  $A_aQ_3\partial_3$  in the operator  $\hat{\partial}_a$  seems not imaginary for the transverse ground state. We expect that cancellation of these terms occurs in matrix elements because of the factor  $\sqrt{\bar{s}}$ .

From Eq. (15), when  $\epsilon \rightarrow 0$ , only  $H_0$  and  $H_1$  survive.  $H_0$  is of the order  $\epsilon^{-1}$ , which describes a particle bounded by the confining potential in the transverse direction and takes a lead role in  $H$ . Being of the order  $\epsilon^0$ ,  $H_1$  corresponds to the quantum dynamics in the tangential direction on  $\mathcal{S}$ . However, we are aiming at investigating the tangential behavior on the surface in the energy range where the quantum particle is in the ground state in the transverse direction. Therefore, the effective Hamiltonian should be of the order  $\epsilon^0$ . To get the effective 2D Hamiltonian we need to consider the Schrodinger equation  $(H_0 + H_1)\Psi = E\Psi$ , where  $E$  denotes the total energy, and separate the wave function.

Taking into account that  $\bar{s}$  is undetermined, we set  $\bar{s} = \sqrt{s}$  and multiply  $1/s$  on both sides of the equation. The equation can be rewritten as follows,

$$\frac{1}{\epsilon}\left[-\frac{\hbar^2}{2m}\partial_3^2 + \frac{m}{2}\omega^2(Q_3)^2\right]\Psi + \frac{H_1}{s}\Psi = \frac{E}{s}\Psi. \quad (18)$$

Formally, this equation is easily separated. If we make the assumption  $\Psi = \psi(q_1, q_2)\chi(Q_3)$ , the usual variable separation gives

$$\left[-\frac{\hbar^2}{2m}\partial_3^2 + \frac{m}{2}\omega^2(Q_3)^2\right]\chi = \epsilon E_0\chi \quad (19)$$

and

$$H_1\psi = (E - sE_0)\psi. \quad (20)$$

It is clear that Eq. (19) describes a one-dimensional harmonic oscillator, and the corresponding energy eigenvalue  $E_0$ , which is of the order  $\epsilon^{-1}$ , is the dominant part of the total energy  $E$ . Equation (20), which describes the 2D effective dynamics on  $\mathcal{S}$  under the transverse mode energy  $E_0$ , can be rewritten as

$$[H_1 + (s - 1)E_0]\psi = E_1\psi, \quad (21)$$

where  $E_1 = E - E_0$ . Here, it should be emphasized that the dynamics separation is based on the perturbative parameter  $\epsilon$ . To ensure the validity of the separation, and taking into account  $E_0 \sim \epsilon^{-1}$ , we have to limit the function  $s(q_1, q_2)$  so that  $(s - 1) \sim \epsilon$ . This limitation also implies the application range of the method. Up to now, we have been able to define

the effective 2D Hamiltonian as

$$H_{\text{eff}} = \int \chi^* [H_1 + (s-1)E_0] \chi dQ_3. \quad (22)$$

Performing the integral in Eq. (22), we eventually obtain the explicit form of the effective Hamiltonian:

$$H_{\text{eff}} = -\frac{\hbar^2}{2m} \frac{1}{\sqrt{g}} \partial_a \sqrt{g} g^{ab} \partial_b + V_g + (s-1)E_0. \quad (23)$$

It should be noted that no gauge potential appears in this effective Hamiltonian, despite the operator  $\hat{\partial}_a$  in Eq. (14) containing the corresponding terms. As expected, this is because the factor  $\sqrt{g}$  in Eq. (17) cancels out these terms after the integration. In contrast to the geometric potential  $V_g$ , the effective potential  $(s-1)E_0$  stemming from the inhomogeneous confinement is relevant to the ground-state energy in the normal direction of the surface. Typically, in a thin-layer system, the thickness  $d$  is much smaller than the curvature radius  $r_c$ . If we set  $\epsilon = d/r_c$ ,  $s-1$  should be of the order  $d/r_c$  at most, which implies that tiny changes in layer thickness can induce considerable influences.

### III. COHERENT TRANSPORT IN A CYLINDER WITH INHOMOGENEOUS CONFINEMENT

Next, we show how the varying thickness of a curved layer affects the transport properties. According to the effective Hamiltonian we have derived, the effective potential induced by the variation of thickness is characterized by the dimensionless function  $s(q_1, q_2)$ . The arbitrary nature of this function allows us to investigate various fluctuations occurring in the thickness of curved nanostructures. Conversely, based on the required form of the effective potential, the thickness distribution on curved surfaces can be designed to confer the corresponding properties on nanostructures. In particular, transport properties of nanostructures are closely related to their geometric symmetries, which can be maintained, reduced, or even totally destroyed according to the features of the thickness variation on curved surfaces.

In this section we give an example of a cylindrical surface with inhomogeneous confining potentials which has helical characters [see Fig. 2(a)]. As shown in the figure, we assume that two-dimensional electron gases are confined to such a cylindrical surface with a radius  $r$ , and the confining potential is homogeneous except two ditches lie in the strip along the green helical lines. Such a structure may be realized by lithography techniques. In this structure, the cylindrical symmetry, which preserves the angular momentum conservation during transmission, is reduced to the chiral symmetry by the helical ditches in thickness.

We suppose that the incident wave goes from the left to the right, and the wave functions of the injection states are  $\psi_{\text{in}} = \frac{1}{\sqrt{2\pi}} e^{i l \theta} e^{i k z}$ , where  $\theta$  is the azimuthal angle and  $k = \sqrt{2m(E_1 - E_l)/\hbar}$ , with  $E_l = \frac{l^2 \hbar^2}{2mr^2}$ . Here,  $E_l = E - E_0$ , with  $E_0$  being the ground-state energy of the quantum well normal to the cylinder in the homogeneous area [ $s(\theta, z) = 1$ ]. For convenience, we scale the length and the energy in units of  $a$  and  $e_0 = \hbar^2/(2ma^2)$ .

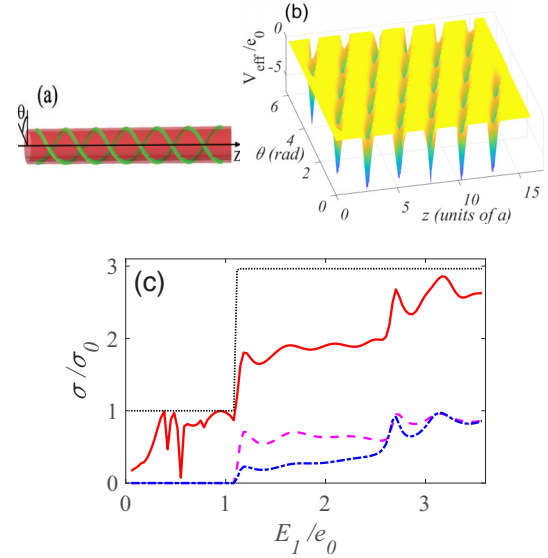


FIG. 2. (a) Schematic of a cylindrical surface. Inhomogeneous confining potentials are arranged along the green helical curves. (b) Effective potential  $E_{\text{eff}}$  in  $(\theta, z)$  coordinates. (c) Conductance ( $\sigma_0 = 2e^2/h$ ) versus energy  $E_l$ . The black dotted line and the red solid line are the total conductance for the cylindrical layer with homogeneous and inhomogeneous confinements, respectively. The pink dashed and blue dash-dotted lines are for the case of injected modes  $l = 1$  and  $l = -1$ , respectively.

To realize an inhomogeneous confinement with helical characteristics, we design the function  $s$  to be

$$s(\theta, z) = 1 - \epsilon \left[ \frac{1}{2} \cos \Omega(r\theta - \kappa z + n\pi) + \frac{1}{2} \right], \quad (24)$$

where  $n = 0, \pm 1, \pm 2, \dots$ ,  $\kappa$  is a parameter to control the tilt angle of the green line in Fig. 2(a) and  $\Omega$  is a parameter to adjust the width of the strips. Such a function describes a slightly weaker confining potential or larger thickness in the strip region. The induced effective potential  $V_{\text{eff}}$  is described in Fig. 2(b) in  $(\theta, z)$  coordinates for  $E_0 = 70e_0$ ,  $\epsilon = 0.1$ , and  $\Omega = 8a^{-1}$ . Such an effective potential leads to the invariance of the Hamiltonian  $H(\theta, z) = H(-\theta, -z)$ , reflecting the chiral symmetry of the system.

By numerically solving the corresponding effective Schrodinger equation, we calculate the transmissions for the modes  $l = 0$  and  $\pm 1$ . Based on the Landauer formula, the conductance at zero temperature is obtained and plotted in Fig. 2(c). We first plot the conductance (black dotted line) for the case that the confinement is homogeneous everywhere, which shows a perfect steplike dependence on  $E_l$ , and the height of the step from  $1\sigma_0$  to  $3\sigma_0$  ( $\sigma_0 = 2e^2/h$  is the quantum of conductance, with  $e$  being the electric charge and  $h$  the Planck constant) indicates that the modes  $l = \pm 1$  are degenerate in this situation. For the inhomogeneous case (red solid line), we observe that the conductance is more complicated and a new plateau of  $2\sigma_0$  from  $1.2e_0$  to  $2.5e_0$  is formed. This plateau shows that the inhomogeneity of the confining potential destroys the degeneracy of the modes  $l = \pm 1$  and only one open channel appears in this energy range. To give a more explicit picture, we draw the conductances for the injected modes  $l = \pm 1$ , where an evident difference between

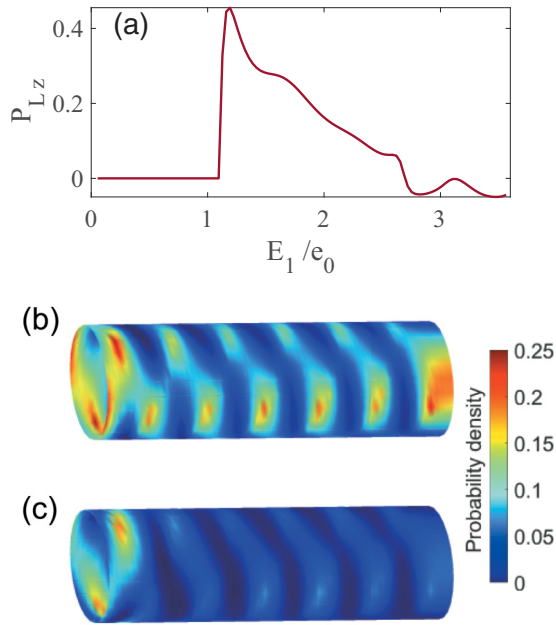


FIG. 3. (a) Mean angular momentum polarization  $P_{Lz}$  of the outgoing current on the right side. (b) and (c) The probability densities for transport when the injected modes are  $l = 1$  and  $l = -1$ , respectively.  $E_1 = 1.3e_0$ .

the two lines emerges, showing that the wave in mode  $l = 1$  is more preferable to pass through the cylindrical structure than that in mode  $l = -1$  in this energy range. As we see, this difference exhibits that the angular momentum is no longer conserved in the transport, which is due to the cylindrical symmetry being reduced to chiral symmetry.

We further define a polarization quantity  $P_{Lz}$  to show the ratio between the mean angular momentum current and the total current, which is

$$P_{Lz} = \sum_{l'} \frac{\sigma_{l',l} - \sigma_{l',-l}}{\sigma}, \quad (25)$$

where  $\sigma_{l',l}$  denotes the conductance that incident modes  $l'$  are scattered into modes  $l$ . In Fig. 3(a) we plot the dependence of  $P_{Lz}$  on the energy  $E_1$ . It shows that once the threshold energy of modes  $l = \pm 1$  is reached, the angular momentum polarization is generated in the outgoing current and has a rapid increase up to a maximum value. With  $E_1$  increasing, the polarization decreases slowly, which is due to the counteraction of the arising conductances  $\sigma_{l',-1}$  carrying the opposite angular momentum. As the chiral symmetry is possessed by the system, it is easy to find that the transmission component  $\sigma_{l',l}$  in the propagation is equal to  $\sigma_{l,l'}$  in the counterpropagation (right to left), which results in the same magnitude but opposite angular momentum polarization for the latter. Such a property can cause angular momentum pumping when

alternating voltage is applied to the system. A similar phenomenon is also found in helical coiled tubes [47], but it is easier and more practical to be realized in cylindrical systems. To visually comprehend the generation of polarization, the probability densities are plotted in Figs. 3(b) and 3(c) at the energy  $E_1 = 1.3e_0$  for the injected modes  $l = 1$  and  $l = -1$ , respectively. We can find that the injected wave in the mode  $l = 1$  is able to be transmitted to the right side, while the wave in the mode  $l = -1$  is mostly reflected.

It should also be noted that the probability density is prominently higher along the helical strips [the green lines in Fig. 2(a)], indicating that a helical and open channel is formed for the mode  $l = 1$ . It demonstrates that by implementing such types of inhomogeneous confinement, it is possible to fabricate 1D waveguides or waveguide lattices on curved surfaces or substrates, which are rarely explored and may be able to show novel phenomena compared to flat cases. It has already been demonstrated theoretically in the optical system that curvature can induce topological phase transition in curved-space lattices [48]. Besides the chiral symmetry, depending on the purpose, we are allowed to design more patterns with various symmetries on the basis of the curved surface, manifesting the interplay between space curvature and lattice models.

#### IV. CONCLUSION

In summary, we have extended the TLP and derived an effective Hamiltonian for a particle constrained to an arbitrary curved surface by inhomogeneous confining potentials. Due to the inhomogeneity of the confinement, we find that an effective potential is induced, which is proportional to the ground-state energy in the normal direction and is also determined by the feature of the confining potential. We apply the method to a cylindrical surface where the confining potential is designed to have two additional helical ditches, and we numerically study the transport properties. It is shown that the helicity of the confinement destroys the degeneration of the excitation modes and leads to the generation of angular momentum polarization in the outgoing current. This method can serve as a tool to conveniently obtain information on energy bands and transport properties for various low-dimensional nanostructures, and enable the designation and ‘writing’ of waveguides on arbitrary geometries.

#### ACKNOWLEDGMENTS

This work is supported in part by the National Natural Science Foundation of China (under Grant No. 12104239), the National Natural Science Foundation of Jiangsu Province of China (under Grant No. BK20210581), the Nanjing University of Posts and Telecommunications Science Foundation (under Grant No. NY221024).

[1] L. A. B. Marcal, B. L. T. Rosa, G. A. M. Safar, R. O. Freitas, O. G. Schmidt, P. S. S. Guimaraes, C. Deneke, and A. Malachias, *ACS Photonics* **1**, 863 (2014).

[2] Z. Ren and P.-X. Gao, *Nanoscale* **6**, 9366 (2014).

[3] Q. Sun, R. Zhang, J. Qiu, R. Liu, and W. Xu, *Adv. Mater.* **30**, 1705630 (2018).

- [4] A. G. Pogosov, A. A. Shevyrin, D. A. Pokhabov, E. Y. Zhdanov, and S. Kumar, *J. Phys.: Condens. Matter* **34**, 263001 (2022).
- [5] V. H. Schultheiss, S. Batz, A. Szameit, F. Dreisow, S. Nolte, A. Tünnermann, S. Longhi, and U. Peschel, *Phys. Rev. Lett.* **105**, 143901 (2010).
- [6] V. H. Schultheiss, S. Batz, and U. Peschel, *Nat. Photonics* **10**, 106 (2016).
- [7] R. Bekenstein, *Nat. Photonics* **11**, 664 (2017).
- [8] J. Zhu, Y. Liu, Z. Liang, T. Chen, and J. Li, *Phys. Rev. Lett.* **121**, 234301 (2018).
- [9] H. T. McMahon and J. L. Gallop, *Nature (London)* **438**, 590 (2005).
- [10] L. Pieuchot, J. Marteau, A. Guignandon, T. Dos Santos, I. Brigaud, P.-F. Chauvy, T. Cloatre, A. Ponche, T. Petithory, P. Rougerie, M. Vassaux, J.-L. Milan, N. Tusamda Wakhloo, A. Spangenberg, M. Bigerelle, and K. Anselme, *Nat. Commun.* **9**, 3995 (2018).
- [11] R. Nishide and S. Ishihara, *Phys. Rev. Lett.* **128**, 224101 (2022).
- [12] Y. Maroudas-Sacks, L. Garion, L. Shani-Zerbib, A. Livshits, E. Braun, and K. Keren, *Nat. Phys.* **17**, 251 (2021).
- [13] K. Horibe, K.-i. Hironaka, K. Matsushita, and K. Fujimoto, *Chaos* **29**, 093120 (2019).
- [14] N. Saito and S. Sawai, *iScience* **24**, 103087 (2021).
- [15] C. Ortix, S. Kiravittaya, O. G. Schmidt, and J. van den Brink, *Phys. Rev. B* **84**, 045438 (2011).
- [16] V. M. Fomin, S. Kiravittaya, and O. G. Schmidt, *Phys. Rev. B* **86**, 195421 (2012).
- [17] C.-H. Chang and C. Ortix, *Nano Futures* **1**, 035004 (2017).
- [18] R. Streubel, F. Kronast, C. F. Reiche, T. Mühl, A. U. B. Wolter, O. G. Schmidt, and D. Makarov, *Appl. Phys. Lett.* **108**, 042407 (2016).
- [19] D. Makarov, O. M. Volkov, A. Kákay, O. V. Pylypovskiy, B. Budinská, and O. V. Dobrovolskiy, *Adv. Mater.* **34**, 2101758 (2022).
- [20] J. Tempere, V. N. Gladilin, I. F. Silvera, J. T. Devreese, and V. V. Moshchalkov, *Phys. Rev. B* **79**, 134516 (2009).
- [21] Z.-J. Ying, P. Gentile, C. Ortix, and M. Cuoco, *Phys. Rev. B* **94**, 081406(R) (2016).
- [22] J. O. Law, J. M. Dean, M. A. Miller, and H. Kusumaatmaja, *Soft Matter* **16**, 8069 (2020).
- [23] H. Jensen and H. Koppe, *Ann. Phys.* **63**, 586 (1971).
- [24] R. C. T. da Costa, *Phys. Rev. A* **23**, 1982 (1981).
- [25] A. Szameit, F. Dreisow, M. Heinrich, R. Keil, S. Nolte, A. Tünnermann, and S. Longhi, *Phys. Rev. Lett.* **104**, 150403 (2010).
- [26] G. Ferrari and G. Cuoghi, *Phys. Rev. Lett.* **100**, 230403 (2008).
- [27] F. T. Brandt and J. A. Sánchez-Monroy, *Europhys. Lett.* **111**, 67004 (2015).
- [28] Y.-L. Wang and H.-S. Zong, *Ann. Phys.* **364**, 68 (2016).
- [29] P. Ouyang, V. Mohta, and R. Jaffe, *Ann. Phys.* **275**, 297 (1999).
- [30] M. Burgess and B. Jensen, *Phys. Rev. A* **48**, 1861 (1993).
- [31] F. Brandt and J. Sánchez-Monroy, *Phys. Lett. A* **380**, 3036 (2016).
- [32] C. Ortix, *Phys. Rev. B* **91**, 245412 (2015).
- [33] M. V. Entin and L. I. Magarill, *Phys. Rev. B* **64**, 085330 (2001).
- [34] J.-Y. Chang, J.-S. Wu, and C.-R. Chang, *Phys. Rev. B* **87**, 174413 (2013).
- [35] Y.-L. Wang, L. Du, C.-T. Xu, X.-J. Liu, and H.-S. Zong, *Phys. Rev. A* **90**, 042117 (2014).
- [36] Y.-L. Wang, H. Jiang, and H.-S. Zong, *Phys. Rev. A* **96**, 022116 (2017).
- [37] G.-H. Liang, Y.-L. Wang, M.-Y. Lai, H. Liu, H.-S. Zong, and S.-N. Zhu, *Phys. Rev. A* **98**, 062112 (2018).
- [38] S. Batz and U. Peschel, *Phys. Rev. A* **78**, 043821 (2008).
- [39] M.-Y. Lai, Y.-L. Wang, G.-H. Liang, F. Wang, and H.-S. Zong, *Phys. Rev. A* **97**, 033843 (2018).
- [40] M.-Y. Lai, Y.-L. Wang, G.-H. Liang, and H.-S. Zong, *Phys. Rev. A* **100**, 033825 (2019).
- [41] P. Maraner and C. Destri, *Mod. Phys. Lett. A* **08**, 861 (1993).
- [42] P. Maraner, *J. Phys. A: Math. Gen.* **28**, 2939 (1995).
- [43] P. Maraner, *Ann. Phys.* **246**, 325 (1996).
- [44] K. Fujii, N. Ogawa, S. Uchiyama, and N. M. Chepilko, *Int. J. Mod. Phys. A* **12**, 5235 (1997).
- [45] P. Schuster and R. Jaffe, *Ann. Phys.* **307**, 132 (2003).
- [46] C. Sheng, H. Liu, Y. Wang, S. N. Zhu, and D. A. Genov, *Nat. Photonics* **7**, 902 (2013).
- [47] G.-H. Liang, Y.-L. Wang, L. Du, H. Jiang, G.-Z. Kang, and H.-S. Zong, *Phys. E (Amsterdam, Neth.)* **83**, 246 (2016).
- [48] E. Lustig, M.-I. Cohen, R. Bekenstein, G. Harari, M. A. Bandres, and M. Segev, *Phys. Rev. A* **96**, 041804(R) (2017).